Catalysis Today 148 (2009) 275–282

Contents lists available at ScienceDirect

Catalysis Today

journal homepage: www.elsevier.com/locate/cattod

Dry reforming of methane in an atmospheric pressure plasma fluidized bed with Ni/γ-Al_2O_3 catalyst

Qi Wang, Yi Cheng *, Yong Jin

Department of Chemical Engineering, Beijing Key Laboratory of Green Reaction Engineering and Technology, Tsinghua University, Beijing 100084, PR China

ARTICLE INFO

Article history:
Available online 5 September 2009

Keywords:
Plasma fluidized bed
Dry reforming
Methane
CO_2
Synergetic effect
Cold plasma

ABSTRACT

The synergetic effect of catalyst and cold plasma on dry reforming of methane was investigated in a plasma fluidized bed with Ni/γ-Al_2O_3 catalyst. As a comparison, the experiments in the plasma packed bed were also carried out. The cold plasma was generated by the dielectric barrier discharge (DBD) at atmospheric pressure. Both contact modes between plasma and catalytic particles promoted the catalyst activity at low temperatures (e.g., 673 K). In the plasma fluidized bed, the synergetic effect of the catalyst and the plasma was clearly identified from 648 K to 798 K. The synergetic effect characterized by the conversion ratio of synergetic results to the sum of the results of only using plasma and only using catalyst showed that the plasma fluidized bed behaved better than the plasma packed bed within a certain temperature range. For the versatile flow regimes in the fluidization of catalysts, the plasma fluidized bed found great potential in plasma enhanced chemical processes by manipulating the gas–solid two-phase flows in the plasma environment.

1. Introduction

The carbon dioxide (CO_2) reforming of methane (CH_4) to produce synthesis gas (H_2, CO) has received much attention for the utilization of both CO_2 and CH_4 resources, especially of the dilute methane resources [1]. However, there are several key issues encountered when using conventional catalysis method to realize the dry reforming process of methane. The main challenge comes from the high-temperature operation, which causes high energy cost, high cost of equipment, and easy deactivation of catalyst due to the carbon deposition or sintering [2–5].

As an alternative, the cold plasma provides a new solution to the direct conversion of CH_4 and CO_2 even at room temperature [6] because the energetic electrons and species in the cold plasma can stimulate the chemical reactions [7–9]. The dielectric barrier discharge (DBD) is often employed to generate the cold plasma since it can be operated at atmospheric pressure [10–12], which has been successfully used in the ozone production and air or water purification [13].

Although the dry reforming of methane can be realized at low temperature without the catalyst, the conversion of reactants and the selectivity to the main products such as carbon monoxide (CO) and hydrogen (H_2) were reported low [7,9,14]. However, many reports showed that the discharge can effectively lower the temperature range of the optimum catalyst performance [15–20]. And our experiments in the plasma packed bed have demonstrated the synergetic effect of the Ni/γ-Al_2O_3 catalyst and the cold plasma for the dry reforming of methane [21]. But to be noted all these synergetic experiments were carried out in the packed bed where the catalytic particles were densely filled in the discharge gap [18,22,23]. The starting point of this work is that the different contact mode between catalyst and cold plasma may bring different combination behavior of these two catalysis manners. Considering the good contact of catalytic particles and gas reactants in a gas–solid fluidized bed, the synergetic effect was investigated in a plasma fluidized bed, i.e., a gas–solid fluidized bed with the imposed plasma effect under atmospheric pressure. It is noted that there are very few investigations about the atmospheric pressure plasma fluidized bed [24,25]. Most of the available reports on plasma fluidized beds involve the vacuum or low-pressure operation, which becomes the major limitation for the further application of the plasma fluidized bed in the process engineering.

In our atmospheric pressure plasma fluidized bed, the cold plasma was generated by the DBD method and the catalytic particles were fluidized in the discharge gap. It was observed that the particle motion in the plasma fluidized bed was significantly influenced by the induced plasma compared to the

* Corresponding author. Tel.: +86 10 62794486; fax: +86 10 62772051.
E-mail address: yicheng@tsinghua.edu.cn (Y. Cheng).

0920-5861/$ – see front matter © 2009 Elsevier B.V. All rights reserved.
doi:10.1016/j.cattod.2009.08.008

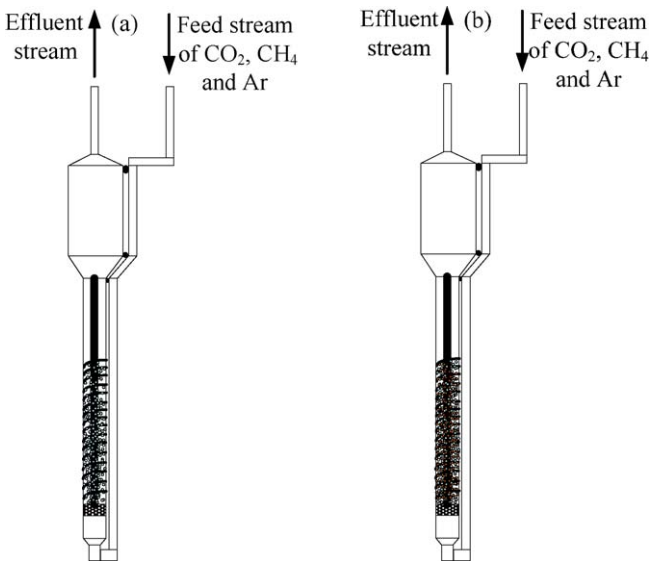

Fig. 1. Schematic diagram of the plasma fluidized bed (shown as (a)), plasma packed bed (shown as (b)).

conventional gas–solid fluidized bed. The plasma fluidized bed was maintained at the bubbling fluidization regime. This work aims to prove the importance of the contact mode between cold plasma and the catalyst. The moving particles in the plasma fluidized bed might bring new features to the synergetic effect of plasma and catalyst. In particular, the operation mode of a plasma fluidized bed would open new areas for plasma-assisted fluidization techniques.

2. Experimental

A schematic diagram of the plasma fluidized bed is shown in Fig. 1(a). The DBD was realized by using a quartz tube as the dielectric medium with the inner diameter of 14 mm. A wire was wrapped around the tube as the outer electrode, and a stainless steel rod acted as the inner electrode with the diameter of 6 mm. As a result, the discharge gap was 4 mm. A thermocouple was inserted into the furnace chamber to measure the environmental temperature around the reactor.

The gas discharge was generated by an AC power amplifier (Nanjing Suman Electronics Corp. CTP-2000K), where the maximum output voltage was 30 kV. The frequency can be adjusted between 1 kHz and 100 kHz. The discharge power of the DBD reactor was calculated according to the *V*–*Q* Lissajous method, as shown in Fig. 2 (see the details described in [6]). All the experiments were carried out at atmospheric pressure. The purity of either CH_4 or CO_2 was 99.999%. The feed rate was controlled by the mass flow controllers (MFCs) with the total flow rate varying from 5 ml/min to 50 ml/min.

The product gases were analyzed by a GC (Shanghai Tianmei Corp.) with a TCD (TDX01 packed column, Lanzhou Chemical Engineering Research Institute) and a FID (HP-plot Al_2O_3 capillary column, Agilent Corp.). The TCD with TDX01 packed column was used to detect the gases of H_2, CO, CH_4 and CO_2, while the FID with HP-plot Al_2O_3 capillary column was used to detect the C1 to C6 hydrocarbons, such as C_2H_6, C_2H_4, C_3H_8, C_3H_6, C_4H_{10}, etc. So the conversion and the selectivity were calculated in terms of Eqs. (1)–(4).

$$C_{CH_4} = \frac{\text{moles of } CH_4 \text{ converted}}{\text{moles of } CH_4 \text{ introduced}} \quad (1)$$

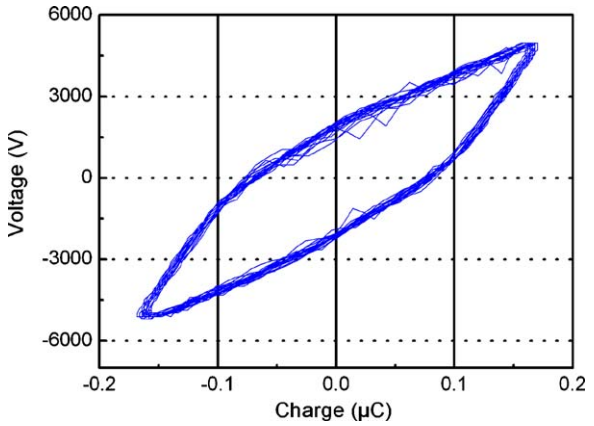

Fig. 2. Calculated discharge power by the *V*–*Q* Lissajous method.

$$C_{CO_2} = \frac{\text{moles of } CO_2 \text{ converted}}{\text{moles of } CO_2 \text{ introduced}} \quad (2)$$

$$S_{CO} = \frac{\text{moles of CO produced}}{\text{moles of } CH_4 \text{ converted} + \text{moles of } CO_2 \text{ converted}} \quad (3)$$

$$S_{H_2} = \frac{\text{moles of } H_2 \text{ produced}}{2 \times \text{moles of } CH_4 \text{ converted}} \quad (4)$$

A commercial catalyst Ni/γ-Al_2O_3 with the NiO concentration greater than 10% was crushed to grains with meshes from 70 to

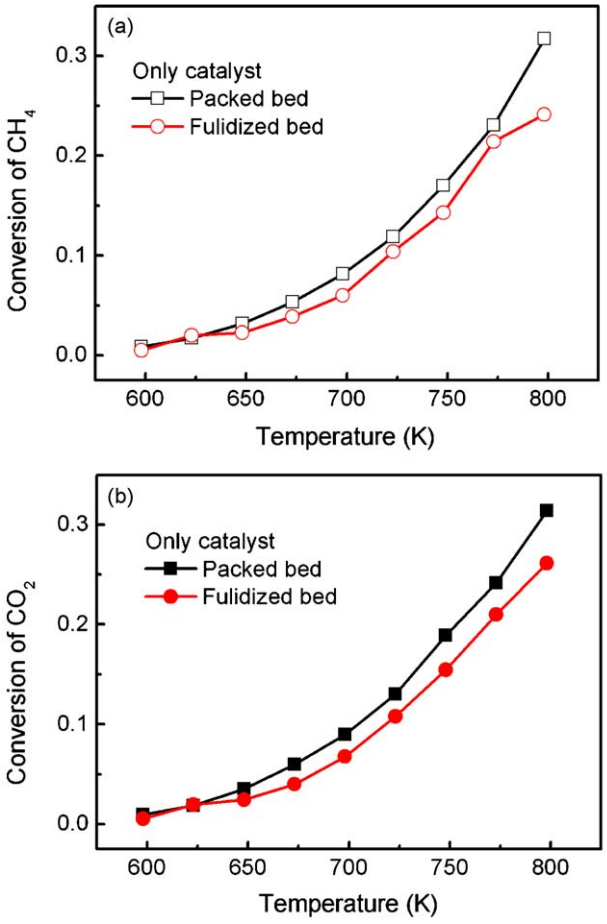

Fig. 3. Performance comparison of CO_2 reforming of CH_4 in terms of reactants' conversions versus the increased temperature under the individual effect of catalyst.

100, and then 10 g catalyst was used in each experiment. The catalyst was reduced at 973 K for 3 h with 10% hydrogen in argon. The characteristics of the catalyst was tested by a JSM 7401F scanning electron microscope (SEM) operated at 3.0 kV and a JEM 2010 transmission electron microscope (TEM) operated at 120 kV, and the element distribution was tested by the energy dispersive X-ray spectrometric microanalysis (EDX). The carbon deposition was tested by a STA 409 PC for thermogravimetry-differential scanning calorimetry (TG-DSC).

The operating condition was fixed at the gas flow rate of 250 ml/min with $CH_4/CO_2 = 1$ and 1282 ml/min argon as the carrier gas. The flux of the carrier gas was determined by maintaining the plasma fluidized bed at the bubbling fluidization regime. Correspondingly, the superficial velocity was 0.2 m/s and the space velocity was 9192 ml/(gCat h), lower than the space velocity commonly used in the conventional catalytic reaction for the dry reforming process. In order to compare the difference of the synergetic effects in a plasma packed bed and in a plasma fluidized bed, the plasma packed bed was also investigated as shown in Fig. 1(b). Five-gram particles of catalyst carrier γ-Al_2O_3 with the same size distribution as the Ni/γ-Al_2O_3 were mixed with the 10 g catalytic particles and fully filled in the discharge gap to keep the same bed height as the plasma fluidized bed. In this way the dry reforming reaction of methane can have the same operation parameters, such as the discharge gap, the input power, the space velocity etc. In order to quantify the synergetic effect, the conversion ratio of the synergetic results using plasma and catalyst to the sum of the results of only using plasma and only using catalyst was defined as I_{SE}, see Eq. (5). The synergetic effect is achieved when I_{SE} is larger than 1. The bed temperature and the input power are the main parameters influencing the synergetic effect of plasma and catalyst.

$$I_{SE} = \frac{\text{conversion using plasma and catalyst}}{\text{conversion with only plasma} + \text{conversion with only catalyst}} \quad (5)$$

3. Results and discussion

3.1. Influence of the bed temperature

To identify the joint effect of catalyst and plasma, experiments were firstly performed with only the plasma discharge at room temperature and only the Ni/γ-Al_2O_3 catalyst versus the increased temperature. Under the individual effect of Ni/γ-Al_2O_3 catalyst, the conversions of both CH_4 and CO_2 in the fluidized bed are the same to that in the packed bed at 598 K and 623 K, then become little lower at or above 648 K as shown in Fig. 3. Under the individual effect of plasma as shown in Fig. 4, where the catalyst has no activity at room temperature, the conversions of both CH_4 and CO_2 in the plasma fluidized bed are lower than that in the plasma packed bed, and the difference becomes much higher with the increase of input power from about 20 W to 90 W. It indicated that the moving particles without catalyst activity were unfavorable to the conversion of reactants by the individual plasma effect. This could be simply explained that the micro-discharge channels

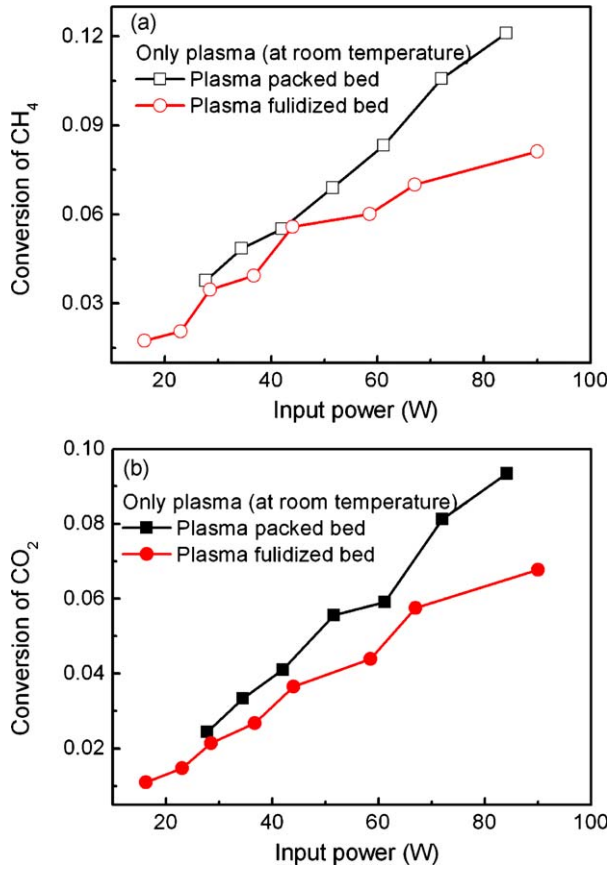

Fig. 4. Performance comparison of CO_2 reforming of CH_4 in terms of reactants' conversions versus the increased input power (at room temperature) under the individual effect of plasma.

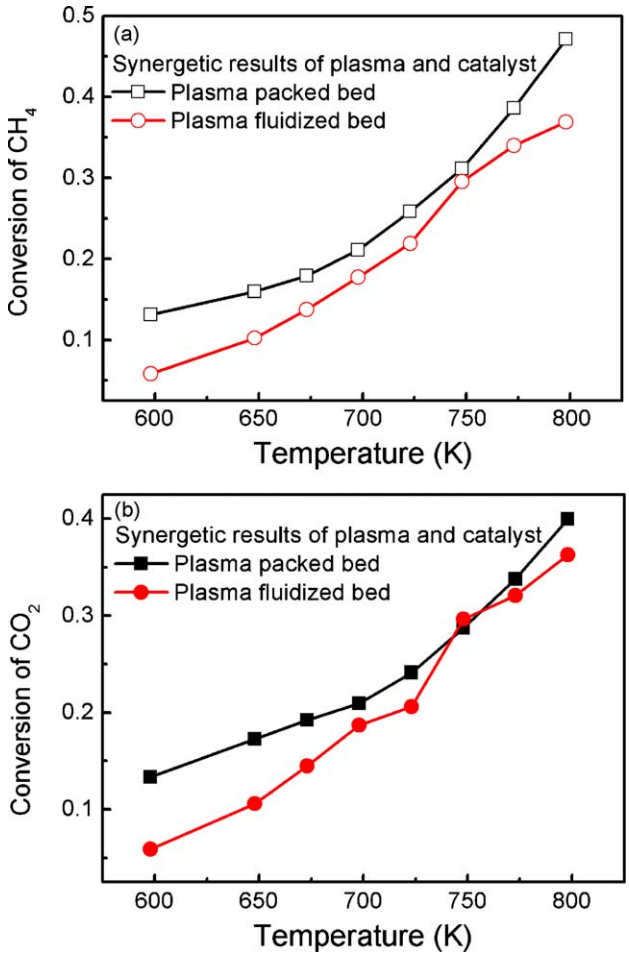

Fig. 5. Performance comparison of synergetic results versus the increased temperature in the plasma fluidized bed and the plasma packed bed.

under the DBD mode are randomly interrupted by the rising or dropping particles, so that the discharge intensity is weakened compared to the stable discharge in the packed bed.

In order to guarantee the comparability of the two kinds of plasma reactors, the synergetic experiments were carried out under the same input power, the same space velocity and the same temperature range. As shown in Fig. 5, the synergetic results of plasma and catalyst in the plasma fluidized bed are little lower than those in the plasma packed bed and nearly the same at 748 K. However, the synergetic effect characterized by I_{SE} presents different performance in the plasma fluidized bed with that in the plasma packed bed (see Fig. 6). In the plasma packed bed, the I_{SE} of CH_4 keeps almost the same with the increase of temperature from 598 K to 798 K, while the I_{SE} of CO_2 decreases from 1.5 to 1.0.

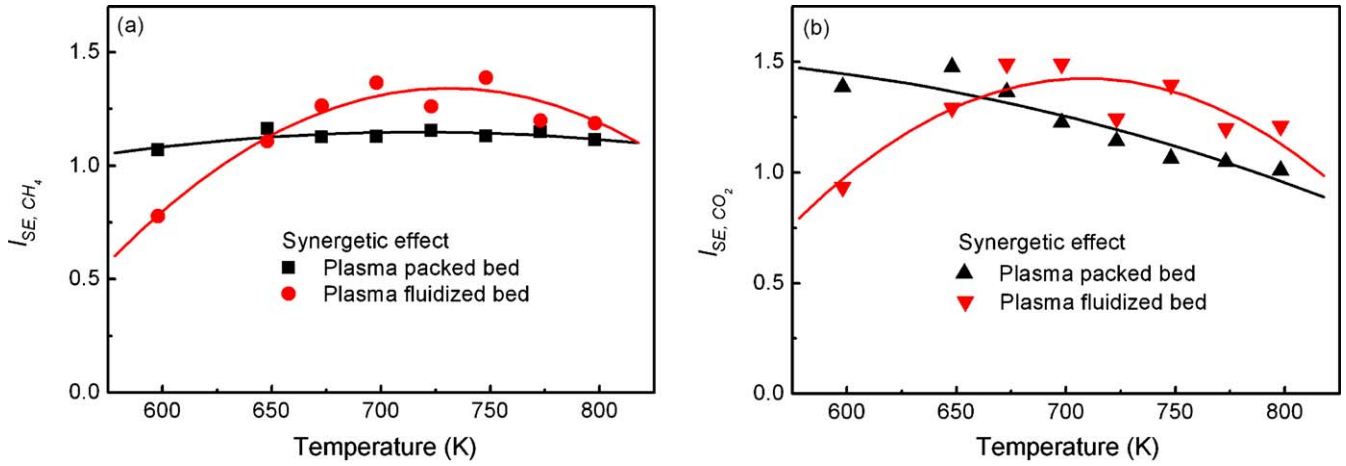

Fig. 6. Comparison of synergetic effect characterized by I_{SE} in the plasma fluidized bed and the plasma packed bed.

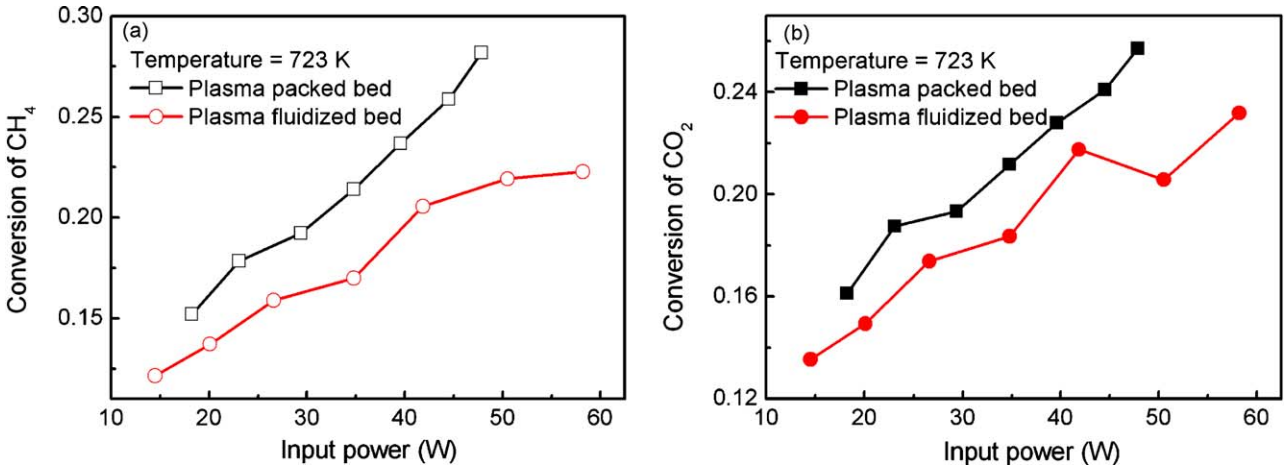

Fig. 7. Performance comparison of the synergetic results versus the increased input power at 723 K in the plasma fluidized bed and the plasma packed bed.

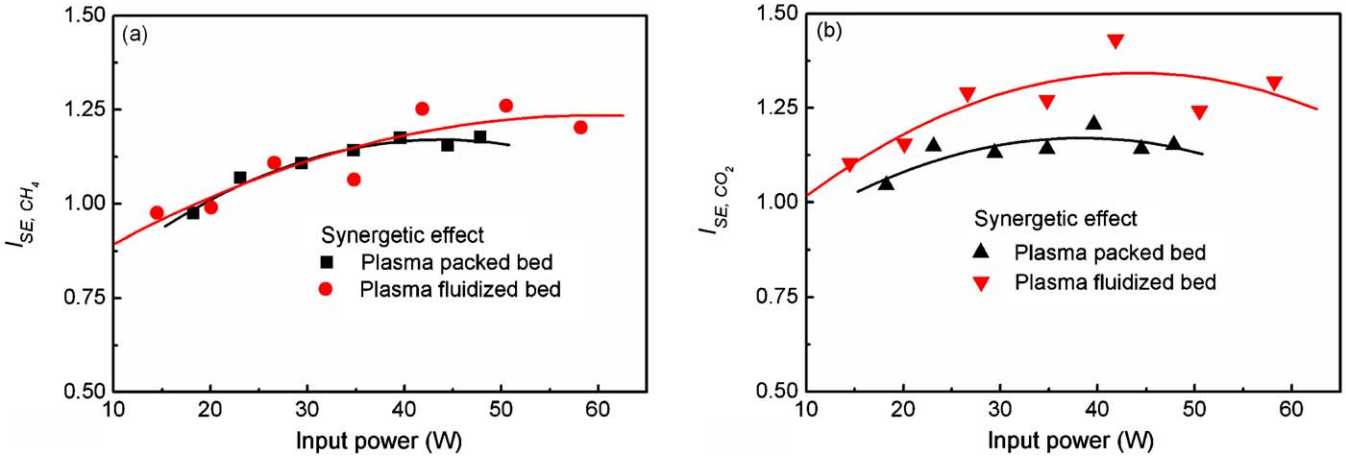

Fig. 8. Comparison of synergetic effect characterized by I_{SE} versus the increased input power at 723 K in the plasma fluidized bed and the plasma packed bed.

However, the I_{SE} is lower in the plasma fluidized bed than that in the plasma packed bed below or at 648 K and becomes higher above 648 K. The I_{SE} of both CH_4 and CO_2 tend to have a maximum between 698 K and 748 K in the plasma fluidized bed, and then decrease with the temperature increase above 748 K. Further, the synergetic effect in the plasma fluidized bed has the trend of lower than that in the plasma packed bed above 798 K according to Fig. 6. These can be concluded that the moving catalytic particles favor to the interaction of plasma and catalyst at a temperature range of 673–798 K and there is an optimal interaction of plasma and catalyst between 698 K and 748 K. Although the rising or dropping catalytic particles would interrupt the micro-discharge channels and decrease the discharge intensity, the catalytic particle traversing the micro-discharge channels has a better interaction and contact efficiency with the plasma when the catalyst is activated with the increased temperature. However, the increase of temperature is unfavorable to the discharge in the DBD reactor, which can explain the decrease of I_{SE} when the temperature increases to a certain range.

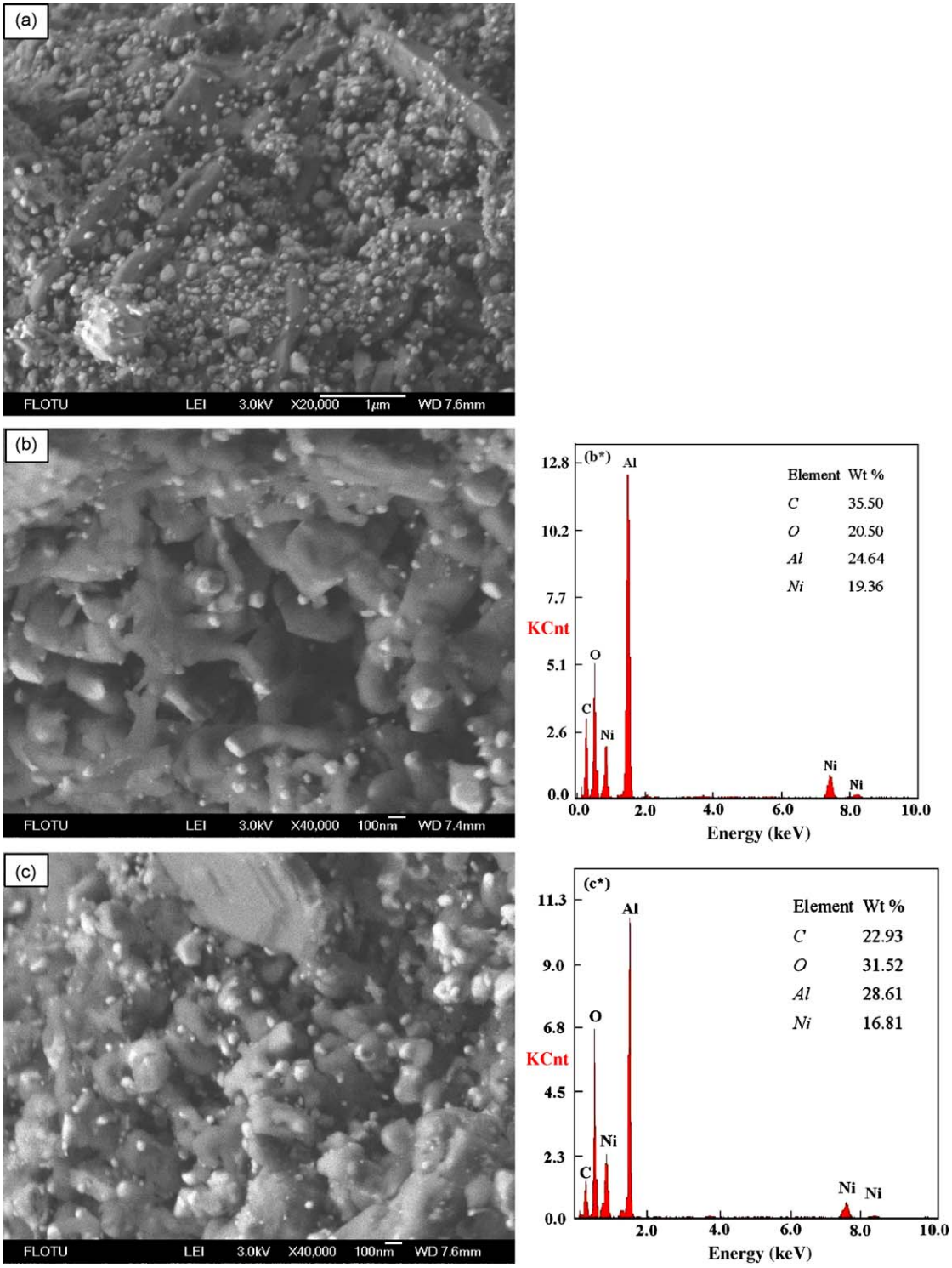

Fig. 9. SEM pictures and EDX of the catalyst surface (a) SEM of the fresh catalyst, (b) SEM of the catalyst after the reaction in the plasma packed bed, (b*) EDX of (b), (c) catalyst after the reaction in the plasma fluidized bed, (c*) EDX of (c).

3.2. Influence of the input power

Another important parameter is the input power. The experiments were done by setting the bed temperature at 723 K and increasing the input power from 15 W to 60 W. As shown in Fig. 7, the conversions of reactants in the plasma fluidized bed are lower than those in the plasma packed bed and increase slower with the increase of input power. However, the I_{SE} of either CH_4 or CO_2 has a similar trend that the I_{SE} increases with the increase of input power (see Fig. 8), except that the I_{SE} of CO_2 presents higher in the plasma fluidized bed than that in the plasma packed bed. This means that the moving catalytic particles favor to intensify the conversion of CO_2 when the catalytic particles traverse the micro-discharge channels instead of the still catalysts.

3.3. Characterization of catalyst after reactions in two kinds of reactors

The dry reforming of methane is a carbon rich reaction, so the carbon deposition is always the main challenge to the catalyst deactivation in this process. Although the catalysis is enhanced by the joint effects of plasma and catalyst compared to the individual effect of catalyst below 798 K, there is still carbon deposition on the catalyst because of the deep cracking of methane and carbon dioxide *catalyzed* by the cold plasma. In particular, the dense

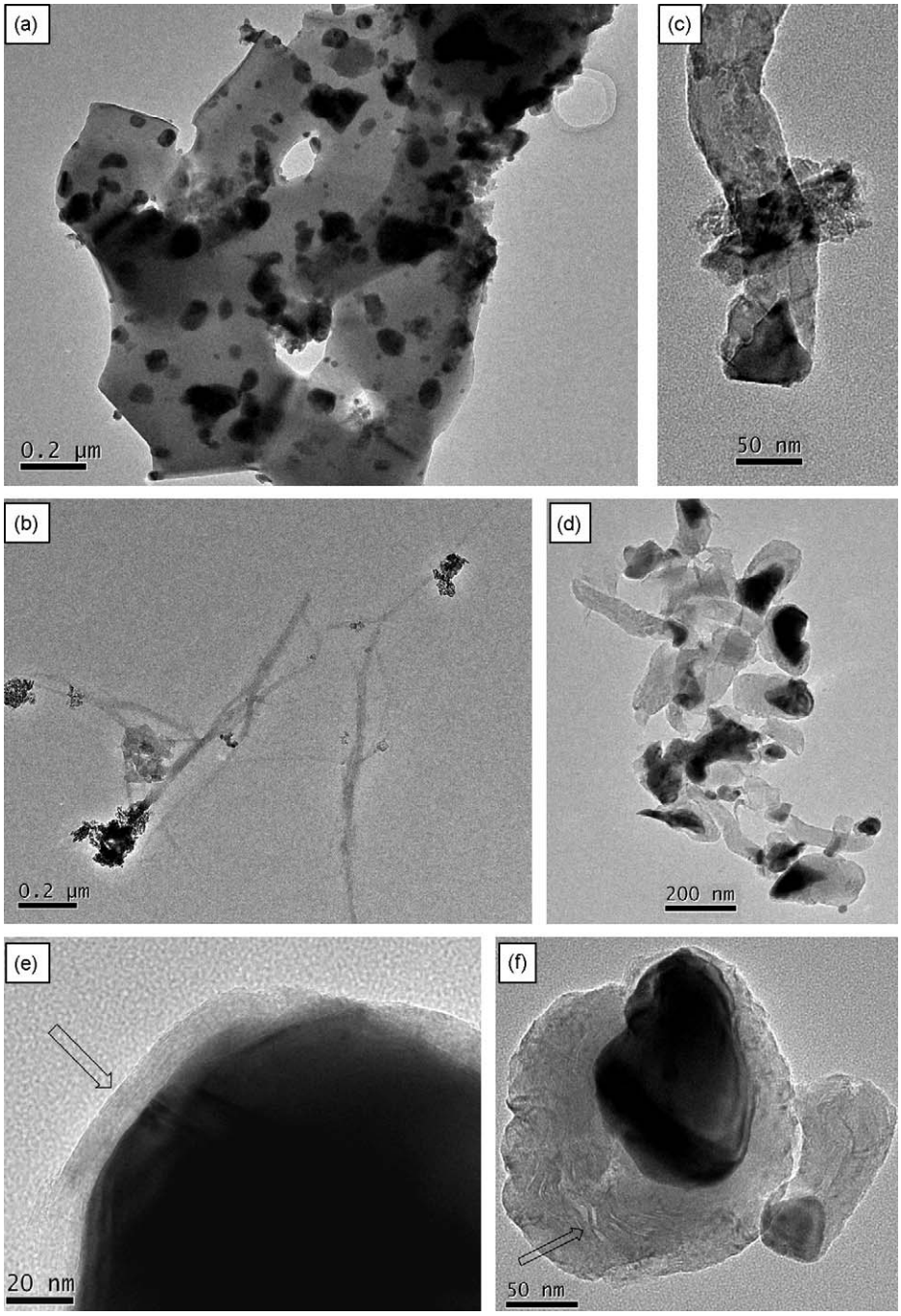

Fig. 10. TEM pictures of the catalyst (a) TEM of the fresh catalyst, (b) TEM of the filamentous carbon on the catalyst after reaction in the plasma packed bed, (c) TEM of the top section of the (b), (d) TEM of the graphite carbon on the catalyst after the reaction in the plasma fluidized bed, (e) and (f) the high resolution of TEM images of the graphite carbon.

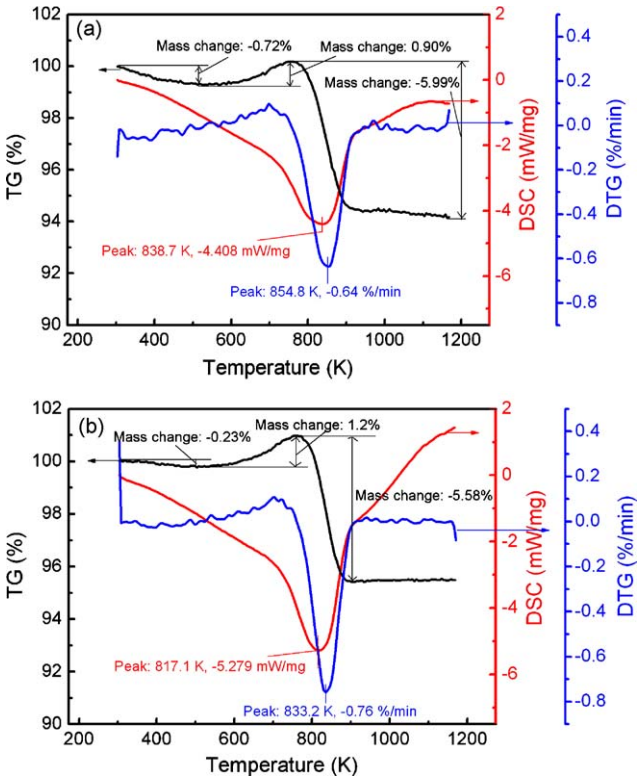

Fig. 11. TG-DSC results (a) catalyst after the reaction in the plasma packed bed (b) catalyst after the reaction in the plasma fluidized bed.

filamentous carbon can be observed on the catalyst after reaction in the plasma packed bed, while a few of filamentous carbon was detected on the catalyst after the same reaction in the plasma fluidized bed (as shown on the SEM pictures with EDX in Fig. 9). This can also be approved by the TEM pictures shown in Fig. 10, where the long filamentous carbon was detected on the catalyst after the reaction in the plasma packed bed (see Fig. 10(b)) and the Ni particle appeared on the top of the filament carbon (see Fig. 10(c)). Also the short filamentous carbon and graphite wrapping the Ni particles can be observed on the catalyst after the reaction in the plasma fluidized bed (see Fig. 10(d)). The flaky graphite can be clearly recognized from the image as the arrow pointed to in Fig. 10(e) and (f). The TG-DSC results of the catalysts after the reaction in the plasma packed bed and plasma fluidized bed show the detailed information of the carbon shown in Fig. 11. The most significant mass decrease section between 750 K and 903 K in both reactors is due to the graphite and filamentous carbon's combustion, which corresponds to the intensively exothermic peak at 854.8 K and 833.2 K, respectively. The first

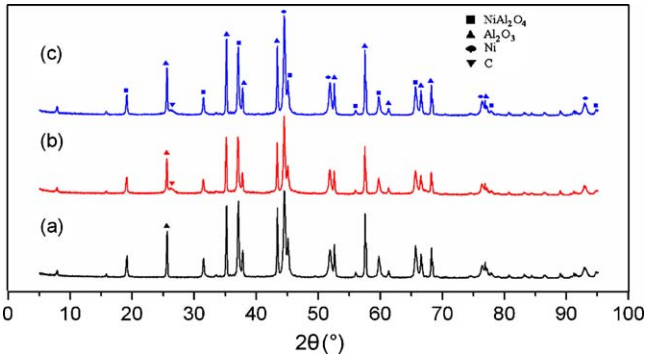

Fig. 12. XRD patterns (a) fresh catalyst (b) catalyst after the reaction in the plasma packed bed (c) catalyst after the reaction in the plasma fluidized bed.

mass decrease around 500 K is due to the removing of the physical adsorbed water and structural water in the catalyst, and the first mass increase peak at nearly 750 K is due to the oxidation of metallic nickel. The XRD patterns of catalysts indicate that there is no sintering happened to the nickel except that the graphite peak was detected at 26° as shown in Fig. 12.

4. Conclusions

Dry reforming of methane was studied in a plasma fluidized bed and a plasma packed bed as well to address the importance of the contact mode between cold plasma and the catalysts. The synergetic effect of catalyst and cold plasma was demonstrated for both contact modes, i.e., for fixed particles and moving ones in the plasma environment, where the optimum temperature range for catalyst activity was lowered from 1073 K to 1173 K without plasma effect to 648–798 K with plasma. However, the plasma fluidized bed behaved differently from the plasma packed bed by the comparison of I_{SE} in these two kinds of reactors. The fluidized catalytic particles favored the interaction between plasma and catalyst at a temperature range between 673 K and 798 K, where a maximum effect existed between 698 K and 748 K. With the increase of the input power, the I_{SE} of CO_2 was higher in the plasma fluidized bed than that in the plasma packed bed, while the I_{SE} of CH_4 was almost the same in these two kinds of reactors. The differences came from the different contact modes of fluidized catalytic particles and settled catalytic particles with the *in situ* cold plasma.

The different type of deposited carbon was observed on the surface of catalyst after the synergetic experiments. The filamentous carbon with Ni particle on the top was the main form of carbon deposition, where the catalyst still kept activity because the Ni exposed outside. However, it might block the tube reactor considering the carbon's accumulation in the catalyst. Therefore, the plasma fluidized bed could be an ideal reactor to decrease the influence of carbon deposition. There was no sintering happened to the nickel when the reaction took place below 798 K.

To sum-up, the moving particles in the plasma fluidized bed might bring new features to the synergetic effect of plasma and catalyst. In particular, the operation mode of a plasma fluidized bed would open new areas for plasma-assisted chemical reactions.

Acknowledgements

Financial support from CNPC Innovation Foundation is acknowledged. The authors would also like to thank the continuous support from PetroChina.

References

[1] A. Rojey, C. Jaffret, S. Cornot-Gandolphe, B. Durand, S. Jullian, M. Valais, Natural Gas: Production, Processing, Transport, Editions TECHNIP, Inc., Paris, 1997, p. 20.
[2] F. Barrai, T. Jackson, N. Whitmore, M.J. Castaldi, Catal. Today 129 (2007) 391.
[3] N.A. Pechimuthu, K.K. Pant, S.C. Dhingra, Ind. Eng. Chem. Res. 46 (2007) 1731.
[4] J.H. Edwards, A.M. Maitra, Fuel Process. Technol. 42 (1995) 269.
[5] A.T. Ashcroft, A.K. Cheetham, M.L.H. Green, P.D.F. Vernon, Nature 352 (1991) 225.
[6] Q. Wang, B.H. Yan, Y. Jin, Y. Cheng, Plasma Chem. Plasma Process. 29 (2009) 217.
[7] B. Eliasson, U. Kogelschatz, IEEE Trans. Plasma Sci. 19 (1991) 1063.
[8] U. Kogelschatz, B. Eliasson, W. Egli, J. Phys. IV 7 (1997) 47.
[9] U. Kogelschatz, Physics and applications of dielectric-barrier discharges, in: IEEE Conference Record – Abstracts, 27th IEEE International Conference on Plasma Science, 2000, p. 81.
[10] L.M. Zhou, B. Xue, U. Kogelschatz, B. Eliasson, Energy Fuels 12 (1998) 1191.
[11] A.M. Huang, G.G. Xia, J.Y. Wang, S.L. Suib, Y. Hayashi, H. Matsumoto, J. Catal. 189 (2000) 349.
[12] M. Kraus, B. Eliasson, U. Kogelschatz, A. Wokaun, Phys. Chem. Chem. Phys. 3 (2001) 294.
[13] J.S. Chang, A.J. Kelly, J.M. Crowley, Handbook of Electrostatic Processes, Marcel-Dekker, Inc., New York, 1995, p. 581.
[14] H.K. Song, H. Lee, J.W. Choi, B.K. Na, Plasma Chem. Plasma Process. 24 (2004) 57.
[15] B. Eliasson, U. Kogelschatz, B.Z. Xue, L.M. Zhou, Ind. Eng. Chem. Res. 37 (1998) 3350.
[16] M.W. Li, Y.L. Tian, G.H. Xu, Energy Fuels 21 (2007) 2335.

[17] X.S. Li, C. Shi, Y. Xu, X.L. Zhang, K.J. Wang, A.M. Zhu, Plasma Process. Polym. 4 (2007) 15.
[18] T. Nozaki, N. Muto, S. Kado, K. Okazaki, Catal. Today 89 (2004) 57.
[19] T. Nozaki, N. Muto, S. Kado, K. Okazaki, Catal. Today 89 (2004) 67.
[20] B. Pietruszka, K. Anklam, M. Heintze, Appl. Catal. A-Gen. 261 (2004) 19.
[21] Q. Wang, B.H. Yan, Y. Jin, Y. Cheng, Energy Fuels 23 (2009) 4196.
[22] M.W. Liu, C.P. Liu, Y.L. Tian, G.H. Xu, F.C. Zhang, Y.Q. Wang, Energy Fuels 20 (2006) 1033.
[23] F. He, C.J. Liu, B. Eliasson, B.Z. Xue, Surf. Interface Anal. 32 (2001) 198.
[24] S.H. Jung, S.M. Park, S.H. Park, S.D. Kim, Ind. Eng. Chem. Res. 43 (2004) 5483.
[25] G. Chen, S. Chen, M. Zhou, W. Feng, W. Gu, S. Yang, J. Phys. D: Appl. Phys. 39 (2006) 5211.